Nuclear Engineering and Technology 54 (2022) 940–947

Contents lists available at ScienceDirect

Nuclear Engineering and Technology

journal homepage: www.elsevier.com/locate/net

Original article

Henry gas solubility optimization for control of a nuclear reactor: A case study

Seyed Mohammad Hossein Mousakazemi

Department of Physics, Faculty of Basic Sciences, Payame Noor University, P.O. Box 19395-4697 Tehran, Iran

ARTICLE INFO

Article history:
Received 11 April 2021
Received in revised form
27 July 2021
Accepted 19 September 2021
Available online 25 September 2021

Keywords:
Pressurized water reactor (PWR)
Proportional–integral–derivative (PID) controller
Henry gas solubility optimization (HGSO)
Point kinetics core model
Lyapunov stability synthesis

ABSTRACT

Meta-heuristic algorithms have found their place in optimization problems. Henry gas solubility optimization (HGSO) is one of the newest population-based algorithms. This algorithm is inspired by Henry's law of physics. To evaluate the performance of a new algorithm, it must be used in various problems. On the other hand, the optimization of the proportional–integral–derivative (PID) gains for load-following of a nuclear power plant (NPP) is a good challenge to assess the performance of HGSO. Accordingly, the power control of a pressurized water reactor (PWR) is targeted, based on the point kinetics model with six groups of delayed-neutron precursors. In any optimization problem based on meta-heuristic algorithms, an efficient objective function is required. Therefore, the integral of the time-weighted square error (ITSE) performance index is utilized as the objective (cost) function of HGSO, which is constrained by a stability criterion in steady-state operations. A Lyapunov approach guarantees this stability. The results show that this method provides superior results compared to an empirically tuned PID controller with the least error. It also achieves good accuracy compared to an established GA-tuned PID controller.

1. Introduction

Recently, meta-heuristic algorithms play an important role in optimization problems. Various algorithms have been developed. Henry Gas Solubility Optimization (HGSO) is one of the newest of them presented by Hashim et al. [1]. This algorithm is inspired by Henry's law of physics. Several studies have also been done based on this algorithm [2–4]. For example, Ekinci et al. used HGSO in several practical applications [5–7]. On the other hand, the optimization of a nuclear reactor control is a good choice to study the efficiency of HGSO. There is no unique criterion for classifying meta-heuristic algorithms, although they can be divided into four main classes based on the sources of inspiration as [1]: (1) swarm intelligence algorithms, such as particle swarm optimization (PSO), and ant colony optimization (ACO); (2) bio-inspired algorithms that referred to as evolutionary algorithms, but not swarm intelligence, such as genetic algorithms (GAs), and evolution strategies (ESs); (3) natural science-based algorithms, which mimic certain chemical laws or physical phenomena, such as gravitational search algorithm (GSA), simulated annealing (SA), heat transfer search, and artificial chemical reaction optimization algorithm (ACROA); and (4) natural phenomena-based algorithms, such as virus colony search, and backtracking optimization search. HGSO belongs to category 3 which mimics Henry's law.

The Proportional–integral–derivative (PID) design with a meta-heuristic algorithm is one of the most popular methods in various industries. For example, İzci and Ekinci [8] performed a comparative performance analysis of the Slime Mould Algorithm (SMA) for the efficient design of PID. İzci et al. [9] used Harris Hawks Optimization (HHO) to tune the PID controller for the aircraft pitch angle control system. Ekinci and Hekimoğlu [10] used an Improved Kidney-Inspired Algorithm for Tuning of PID in AVR microcontroller.

Various studies have been performed on the power control of the nuclear power plant (NPP). Mousakazemi et al. [11,12] used a GA and a PSO algorithm to tune the PID gains in the control of a pressurized water reactor (PWR) based on the point kinetics model with three groups of the delayed-neutron precursors. They used these optimization algorithms for power level control in load-following scenarios. Wan and Zhao [13] designed a two-degree-of-freedom controller for a PWR. They used the effect of model parameter changes based on a linearized transfer function of the one-group delayed neutron model. Elsisi and Abdelfattah [14] designed an optimal variable structure controller with the lightning search algorithm. Their method was used for the feedback, and the

E-mail addresses: smh_mousakazemi@pnu.ac.ir, mousakazemi@gmail.com.

https://doi.org/10.1016/j.net.2021.09.029

sliding equation gains tuning. They also compared the proposed method with GA optimization. Puchalski et al. [15] proposed a fuzzy multi-regional fractional order PID controller for load-following of a PWR NPP, based on two-stage tuning methods. They used direct search optimization to tune the fuzzy controller. Also, meta-heuristic algorithms have been widely used in the nuclear power plant industry. Meneses et al. [16] used PSO, cross-entropy algorithm (CE), artificial bee colony (ABC), and population-based incremental learning (PBIL) to optimize the loading pattern of an NPP. The optimization results of these four codes compared with each other and with the RECNOD code. Ortiz-Servin et al. [17] presented a methodology to optimize integrated fuel lattice and fuel load with a population-based meta-heuristic algorithm for a boiling water reactor (BWR). This algorithm optimized the sets of potential fuel lattice and fuel reload in parallel. Wrigley et al. [18] optimized the module layout of a light water modular NPP with GA. They reviewed the arrangement of plant modules in balance. The result showed a reduction in NPP costs. Lim et al. [19] designed cask shielding with PSO for a prototype sodium-cooled fast reactor. PSO was used to yield optimum shielding thickness versus cask weight. In the field of nonlinear research in the nuclear industry, Zare et al. [20] used a fractional nonlinear model to design the robustness of an optimized FPID controller against uncertainty and disturbance for a research nuclear reactor. Wang et al. [21] proposed a nonlinear adaptive sliding mode control strategy for modular high-temperature gas-cooled reactors. Kastin et al. [22] studied nonlinear stability and limit cycles in xenon-induced reactor oscillations.

HGSO as a novel meta-heuristic algorithm has been used to tune PID gains for a load-following operation of a typical PWR nuclear reactor. The dynamics of nuclear reactors are nonlinear, which makes it very difficult to use analytical methods. This optimization algorithm is inspired by Henry's law, which focuses on the gas solubility into a liquid. The advantage of this algorithm is the balance between exploration and extraction in the search space, and good performance to avoid a local optimum. An algorithm with these features and within an important application problem is the contribution of this study. Rapid changes in the output are more effective for checking the quality of control in terms of overshoot or undershoot and error integral criteria. Accordingly, in this study, fast power transient is considered. Besides, the delay effect of neutron poisons such as xenon can be ignored in rapid power changes. So, the point kinetics model can be relatively valid. It should be noted that the main purpose of this study is to investigate the quality and performance of the novel optimization method in an established model of a reactor core. In some mentioned researches and many other studies, the linearization of the nonlinear equations has been used to obtain a transfer function, which reduces the accuracy of the results. Whereas in this work, the real model is used in optimization and simulation. In some works, one group and three groups of delayed-neutron precursors have been used, while in this study six groups of delayed-neutron precursors are used.

2. Materials and methods

2.1. Nuclear dynamics model

A 12th order dynamics model is considered for the proposed control system. In this model, the point kinetics of a typical PWR NPP is used, with six groups of delayed-neutron precursors. Also, the reactivity feedback which is used includes xenon, lumped fuel temperature, and lumped coolant temperature effects, as follows [23]:

$$\frac{\mathrm{d}n_r}{\mathrm{d}t}=\frac{\rho-\beta}{\Lambda}n_r+\sum_{i=1}^{6}\frac{\beta_i}{\Lambda}c_{ri} \tag{1}$$

$$\frac{dc_{ri}}{dt}=\lambda_i n_r-\lambda_i c_{ri},\ \ (i=1,2,\ldots 6) \tag{2}$$

where n_r: neutron density relative to initial equilibrium density (n_0); c_r: precursor density relative to initial equilibrium density (c_0); ρ: total reactivity, $\delta k/k$; β_i: ith group effective delayed-neutron fraction; β: effective delayed-neutron fraction, $\beta=\sum_{i=1}^{6}\beta_i$; Λ: neutron generation time, s; and λ_i: ith delayed-neutron group decay constant, s^{-1}.

$$\frac{dXe}{dt}=\left(\gamma_{Xe}\Sigma_f-\sigma_{Xe}Xe\right)\frac{P_0}{G\Sigma_f V}n_r-\lambda_{Xe}Xe+\lambda_I I \tag{3}$$

$$\frac{dI}{dt}=\gamma_I\Sigma_f\frac{P_0}{G\Sigma_f V}n_r-\lambda_I I \tag{4}$$

where Xe: xenon concentration, cm^{-3}; γ_{Xe}: xenon yield per fission; λ_{Xe}: xenon decay constant, s^{-1}; I: iodine concentration, cm^{-3}; γ_I: iodine yield per fission; λ_I: iodine decay constant, s^{-1}; P_0: rated power, MW; G: useful thermal energy liberated per fission of $_{235}U$, MW·s; Σ_f: macroscopic thermal neutron fission cross-section, cm^{-1}; and V: core volume, cm^3.

$$\frac{dT_f}{dt}=\frac{1}{\mu_f}\left[f_f P_0 n_r-\Omega T_f+\frac{1}{2}\Omega T_e+\frac{1}{2}\Omega T_l\right] \tag{5}$$

$$\frac{dT_l}{dt}=\frac{1}{\mu_c}\left[\left(1-f_f\right)P_0 n_r+\Omega T_f-\frac{(2M+\Omega)}{2}T_l+\frac{(2M-\Omega)}{2}T_e\right] \tag{6}$$

where T_f: fuel average temperature, $^\circ C$; T_l: coolant outlet temperature, $^\circ C$; T_e: coolant inlet temperature, $^\circ C$; μ_f: fuel total heat capacity, MW·s/$^\circ C$; μ_c: coolant total heat capacity, MW·s/$^\circ C$; f_f: fraction of reactor power deposited in the fuel; Ω: coefficient of heat transfer between fuel and coolant, MW/$^\circ C$; and M: mass flow rate time heat capacity of water, MW/$^\circ C$.

$$\frac{d\rho_r}{dt}=G_r Z_r \tag{7}$$

$$\rho=\delta\rho_r+\alpha_f\left(T_f-T_{f0}\right)+\alpha_c(T_c-T_{c0})-\alpha_{Xe}(Xe-Xe_0) \tag{8}$$

where G_r: control rod total reactivity, $\delta k/k$; Z_r: control rod speed, fraction of core length/s; δ_r: reactivity due to control rod movement, $\delta k/k$; T_{f0}: fuel average temperature at the initial condition, $^\circ C$; T_{c0}: coolant average temperature at the initial condition, $^\circ C$; Xe_0: xenon concentration at the initial condition, cm^{-3}; α_f: fuel temperature coefficient, $(\delta k/k)/^\circ C$; α_c: coolant temperature coefficient, $(\delta k/k)/^\circ C$; and α_{Xe}: xenon coefficient, $(\delta k/k)\cdot cm^3$.

2.2. Stability condition

In this study, a Lyapunov approach is considered as a constraint in the optimization algorithm. The Lyapunov-like function is used as follows [24]:

$$V = \frac{1}{2}e^2 \tag{9}$$

where $e(t)$ is the tracking error between the output and the desired signal.

Lyapunov-like function derivative is as follows, which must be negative in terms of control laws.

$$\dot{V} = \dot{e} \cdot e \tag{10}$$

where $\dot{e}$ is the tracking error derivative.

The negation of this function indicates that the Lyapunov function is finite, and therefore the stability condition is realized.

2.3. Henry Gas Solubility Optimization (HGSO)

The new HGSO meta-heuristic algorithm has been introduced by Hashim et al. [1]. In this law of physics, the amount of gas that dissolves in a certain amount of a liquid is directly proportional to the partial pressure of that gas on top of the solution at a constant temperature. This can be expressed as follows [1]:

$$S_g = k_H P_g \tag{11}$$

where S_g: gas solubility; k_H: Henry's constant of a certain gas-solvent combination at a specific temperature; and P_g: partial pressure.

Fig. 1 shows the solubility of gas particles due to two different pressures, which signifies the principle of Henry gas solubility [1].

Henry's constant is strongly dependent on temperature and must be considered. The Van't Hoff equation describes this effect as follows [1]:

$$\frac{d\ln k_H}{d(1/T)} = -\frac{\nabla_{sol}E}{R} \tag{12}$$

where $\nabla_{sol}E$: dissolution enthalpy; R: gas constant; and T: temperature.

Therefore, the following amendment can be included in Eq. (11) [1]:

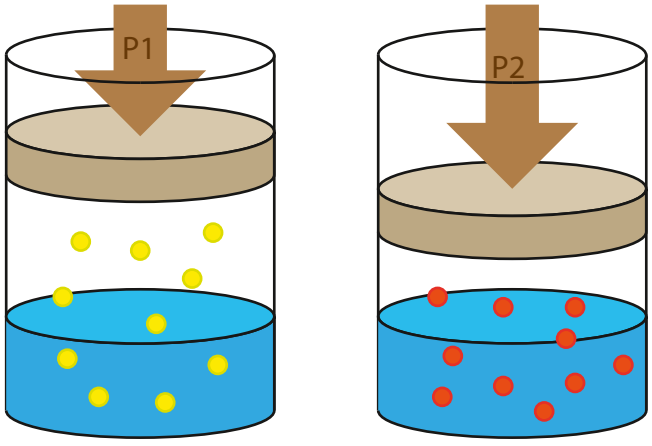

Fig. 1. Partial pressure effect on the solubility of a gas in a liquid [1].

$$k_H(T) = A \times e^{B/T} \tag{13}$$

where A and B are two temperature-dependent factors.

An alternative formula can be expressed for k_H as Eq. (14), based on the reference temperature $T_0 = 298.15$ K [1].

$$k_H(T) = k_{0_H} \times e^{\frac{-\nabla_{sol}E}{R}\left(\frac{1}{T}-\frac{1}{T_0}\right)} \tag{14}$$

where k_{0H}: Henry's constant of a certain gas-solvent combination at the reference temperature.

The validity of the Van't Hoff equation is based on the constant $\nabla_{sol}E$. Accordingly, Eq. (14) is modified as follows [1]:

$$k_H(T) = k_{0_H} \times e^{-C\left(\frac{1}{T}-\frac{1}{T_0}\right)} \tag{15}$$

2.3.1. Algorithm

The mathematical model of this algorithm consists of 8 steps [1]:

Step 1: The population of gases and their positions are generated randomly as follows:

$$X_i^t = X_{min} + U(0,1) \times (X_{max} - X_{min}),\ (i = 1, 2, \ldots, n_{pop}) \tag{16}$$

where X_i^t: ith gas of population; t: iteration (generation) index; n_{pop}: population number; X_{min}: lower bound of solution space; X_{max}: upper bound of solution space; and $U(0,1)$: uniform random number generator.

Also, the properties of each gas are defined as follows:

$$\begin{cases} k_{H_j}^t = l_1 \times U_1(0,1) \\ P_{i,j}^t = l_2 \times U_2(0,1) \\ C_j^t = l_3 \times U_3(0,1) \end{cases} \tag{17}$$

where $k_{H_j}^t$: Henry's constant for jth cluster type in iteration t; $P_{i,j}^t$: partial pressure of ith gas in jth cluster in iteration t; C_j^t: $(= \nabla_{sol}E/R)$ constant value of jth cluster type in iteration t; $U(0,1)$: uniform random number generators; and l: constant values.

Step 2: Gases in the population are distributed into clusters with equal members. Henry's constant value of gases in each cluster $(k_{H_j}^t)$ is fixed due to the similarity of its gases.

Step 3: Gases are evaluated in clusters based on an objective (cost) function. A gas with the best cost/fitness is selected in each cluster, i.e. $X_{j,best}$. Then, the global best of the population is selected among the best gas of clusters, i.e. X_{best}.

Step 4: Since the temperature is changed in each iteration, it is necessary to update Henry's constant as follows [1]:

$$k_{H_j}^{t+1} = k_{H_j}^t \times e^{-C_j \times (1/T^t - 1/T^0)},\ T^t = e^{\frac{-t}{n_{iter}}} \tag{18}$$

where $k_{H_j}^{t+1}$: Henry's constant of jth cluster in new generation $t+1$; T^t: temperature of the iteration t; and n_{iter}: number of algorithm iteration.

Step 5: Meanwhile, the ith gas solubility of the jth cluster should be updated as follows [1]:

$$S_{i,j}^t = \kappa \times k_{H_j}^{t+1} \times P_{i,j}^t \tag{19}$$

where κ is a constant value.

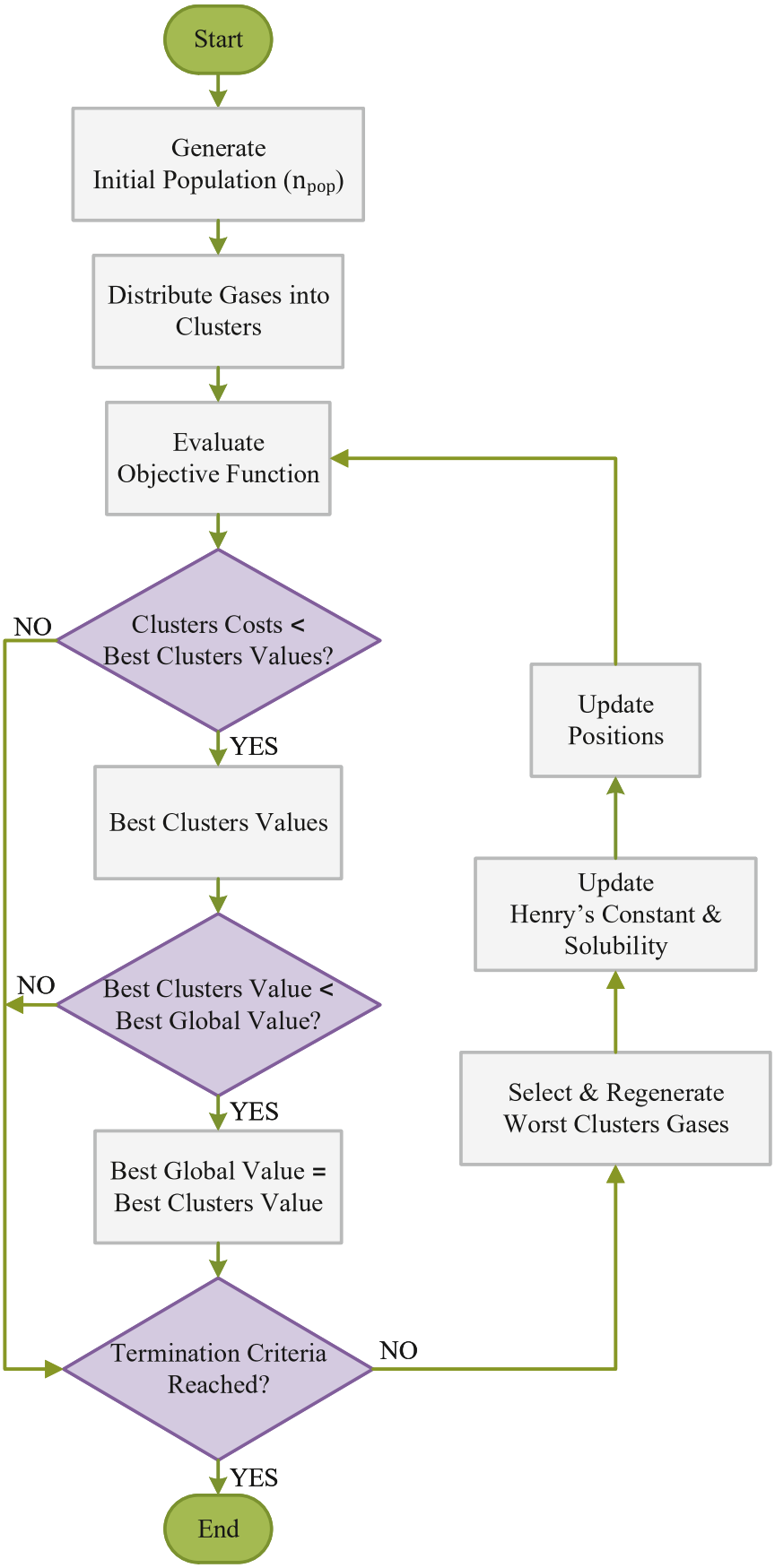

Fig. 2. HGSO flowchart.

Table 1
HGSO parameters.

Parameters	Value
Members of each gas	k_P, k_I, k_D
Maximum Iteration	150
population size (n_{pop})	30
X_{min}	0
X_{max}	1
l_1	0.05
l_2	100
l_3	0.01
κ	1
α	1
ξ	1
ε	0.05
c_1	0.1
c_2	0.2

Step 6: After updating the properties of gases, the ith gas position of the jth cluster is updated in new generation $t+1$ as follows [1]:

$$X_{i,j}^{t+1} = X_{i,j}^{t} + F \times U_1'(0,1) \times \gamma \times \left(X_{j,best} - X_{i,j}^{t}\right) + F \times U_2'(0,1) \times \alpha \times \left(S_{i,j}^{t} \times X_{best} - X_{i,j}^{t}\right), \gamma = \xi \times e^{-\left(F_{best}^{t} - \varepsilon\right)/\left(F_{i,j}^{t} + \varepsilon\right)} \tag{20}$$

where γ: ability of ith gas in jth cluster to interact with each other; F: $(=\pm)$ a flag to control search direction and provides diversity; α: influence of other gases on ith gas; ξ: a constant value; $U'(0,1)$: uniform random number generators; $F_{i,j}^{t}$: best cost/fitness of ith gas in jth cluster; F_{best}^{t}: global best cost/fitness value; and ε: a constant with a small value to avoid the error of dividing by zero.

Step 7: On the other hand, heuristic algorithms may be optimized locally. Therefore, several worst solutions (N_w) are selected based on the following expression [1]:

$$N_W = n_{pop} \times [U''(0,1) \times (c_2 - c_1) + c_1] \tag{21}$$

where $U''(0,1)$: uniform random number generator; and c: constant value.

Step 8: Then, the positions of the worst gases are regenerated by Eq. (16).

In subsequent iterations, this process is followed from step 3 until the termination criteria are reached.

The HGSO flowchart is briefly illustrated in Fig. 2.

The coefficients n_{pop}, n_{iter}, X_{min}, X_{max}, l_1, l_2, l_3, κ, α, β, ε, c_1, and c_2 of HGSO algorithm in this work, are presented in Table 1.

2.3.2. Objective function definition

An objective (cost) function is considered to evaluate gases. The ITSE performance index is a proper option for PID gains tuning as a valid method. ITSE is widely used in the literature and incorporates transient response performance criteria [25–30]. On the other hand, to evaluate the performance of a new optimization method, an established performance index such as ITSE is a good choice. In this study, this performance index is defined as follows:

$$ITSE = \int_0^{\infty} te^2(t)\mathrm{d}t \tag{22}$$

Besides, the stabilization time (St_Time) is added to the objective (cost) function, only in the output steady-state. This time is gained from the constraint of the Lyapunov approach, as mentioned in section 2.2. As mentioned in Section 2.2, if the derivative of the Lyapunov function ($\dot{V}$) is negative, the Lyapunov function is bounded. Accordingly, the Lyapunov function (V) has alternating positive and negative values in desired zones (steady-states). But at a certain time, its value is negative and will remain negative until the end of that desired zone. This time has been named stabilization time (St_Time). Therefore, the stability condition is guaranteed according to Lyapunov synthesis. Shortening (cost) of this stabilization time is important. It is therefore added as a constraint to the performance index (ITSE). The weighted ITSE (multiply by 1000) and the stabilization time have formed the objective (cost) function as follows:

$$Cost = ITSE + St\_Time \tag{23}$$

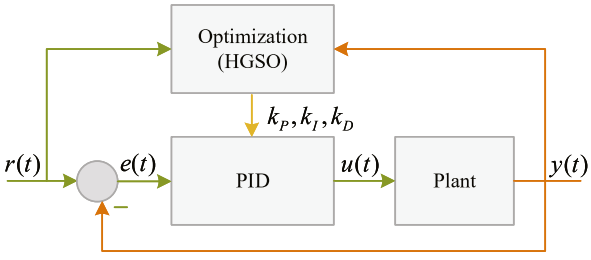

Fig. 3. The diagram of the HGSO–PID control system, where $r(t)$: desired signal; $y(t)$: plant output signal; and $u(t)$: controller signal.

2.4. HGSO–PID control system

The standard PID controller is used, which is popular in industries, especially in NPPs. This controller operates on the tracking error between the output and the desired signal as follows [31]:

$$u(t) = k_P e(t) + k_I \int_0^t e(\tau)\mathrm{d}\tau + k_D \frac{\mathrm{d}}{\mathrm{d}t} e(t) \tag{24}$$

HGSO script code is joined to the PID as Fig. 3. The optimization procedure (HGSO) calculates the best PID gains in each time zone of power level. The optimization process is completed separately in each zone until the last algorithm iteration. The controller and reactor model are simulated by the MATLAB/Simulink environment based on PID gains generated by HGSO in each zone and iteration. The simulation outputs are fetched by a script code related to HGSO and ITSE is calculated. The stabilization time is estimated by the stability condition (Section 2.2.). This time is summed with ITSE to form and evaluate the cost function. Gases are PID gains that are ranked based on cost function values and the best gas in each cluster and the global is selected at each iteration (Fig. 2). This process is called HGSO–PID.

3. Results and discussion

To study the power level control performance under the action of the proposed HGSO–PID, simulations are conducted in the MATLAB/Simulink environment. The initial output power level of the PWR is assumed at nominal power ($n_r = 1$). The power demand changes from 100% → 30% → 100% with a rate of 12%/min. The rapid power changes lead to increased overshoot. As a result, it better shows the performance of the HGSO–PID control system. The analytical results of the optimizations are given in Table 2 for four time zones of power level changes. The stabilization time (St_Time) in the steady-state zones (2 and 4) occurs in short times, and until

Table 2
Analytical results of the simulations.

Parameters	zone 1	zone 2	zone 3	zone 4
Time intervals (s)	150 – 500	500 – 700	700 – 1050	1050 – 1200
k_P	1	0.995656345	1	0.705241035
k_I	1	0.586175975	1	0.329062908
k_D	1	0.042879083	1	0.998530689
Overshoot/Undershoot[a]	0.504873×10^{-3}	1.853709×10^{-3}	1.289464×10^{-3}	0.900836×10^{-3}
Settling time (s)	0	0	0	0
Rise time (s)	0	0	0	0
St_Time (s)	–	20.887	–	15.732
Steady-state error[b]	9.20675×10^{-6}	0.25886×10^{-6}	3.32967×10^{-6}	0.37464×10^{-6}
ITSE	0.101826×10^{-3}	4.934787×10^{-3}	3.227548×10^{-3}	4.139781×10^{-3}
Best Cost	0.101825708	25.82178665	3.227548248	19.87178081

[a] In ramps, a maximum derivation from the desired signal.
[b] In ramps, the latest error.

the end of that zone, the derivative of the Lyapunov function will remain negative. Therefore, stable conditions will be guaranteed. Also, it should be noted that in the ramp zones, the algorithm has reached its maximum possible position value to attain the optimal response due to the continuous change of the output level. Fig. 4 shows the output results of the HGSO–PID control system in the form of the relative neutron density, which is compared with the GA–tuned and an empirically tuned PID controller (named Not-tuned PID). We know that the relative neutron density is equivalent to the relative power changes.

The convergence of the best cost function can show the accuracy of optimization algorithms. Fig. 5 shows the best cost over time in steady-state zones (2 and 4), besides this convergence is seen in each of them. In the ramp zones (1 and 3), HGSO has reached the best cost with the initial population and has not improved in the next iterations.

Fig. 6 shows the control rod speed in this transient. The result shows a maximum peak of 1.43cm/s (based on the core height) in 700 s, which is a small amount. Therefore, there is no need for extreme control. Also, there is no rapid change of the control rod that may make it difficult to operate on hardware actuators.

Fig. 7 shows the reactivity induced by the control rod movement. Its behavior follows the desired relative neutron density well. Also, it is observed that the reactor is well-controlled in all zones with one control rod bank.

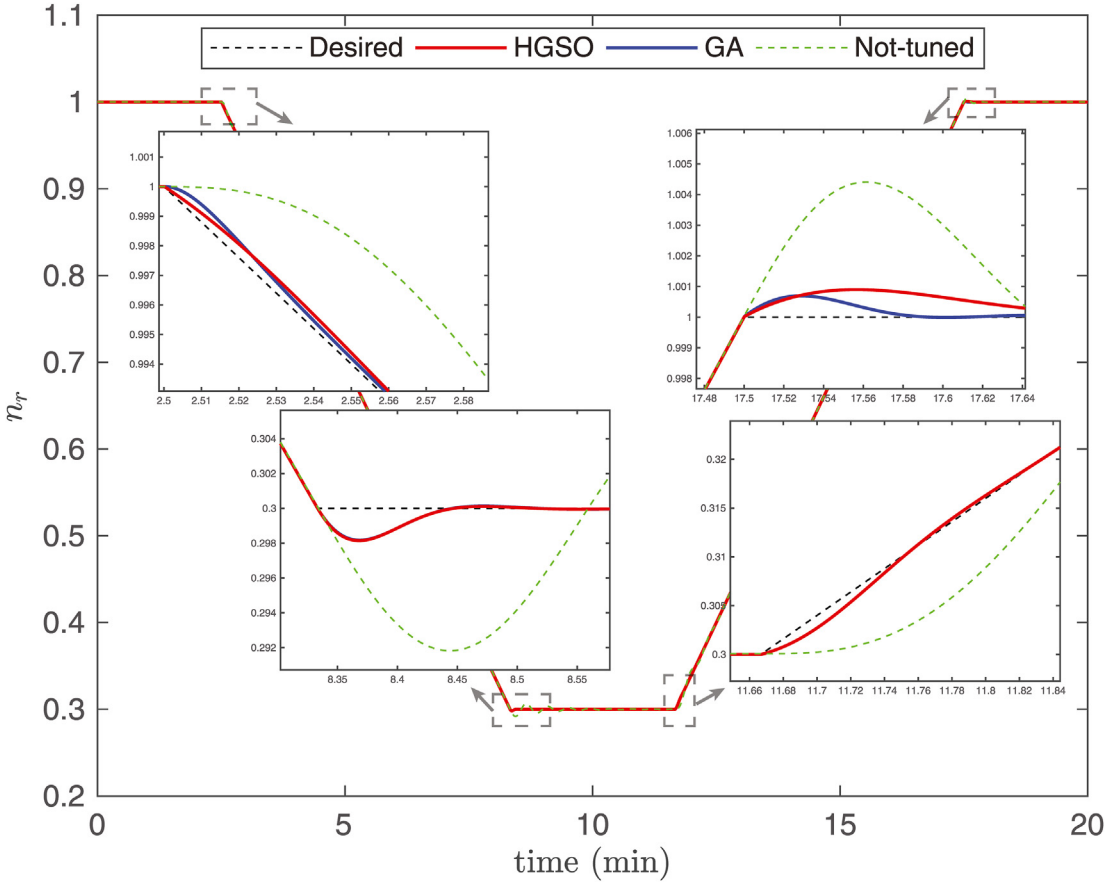

Fig. 4. Relative neutron density for the HGSO–PID control system, GA-tuned PID controller, and an empirically tuned PID controller (named Not-tuned PID).

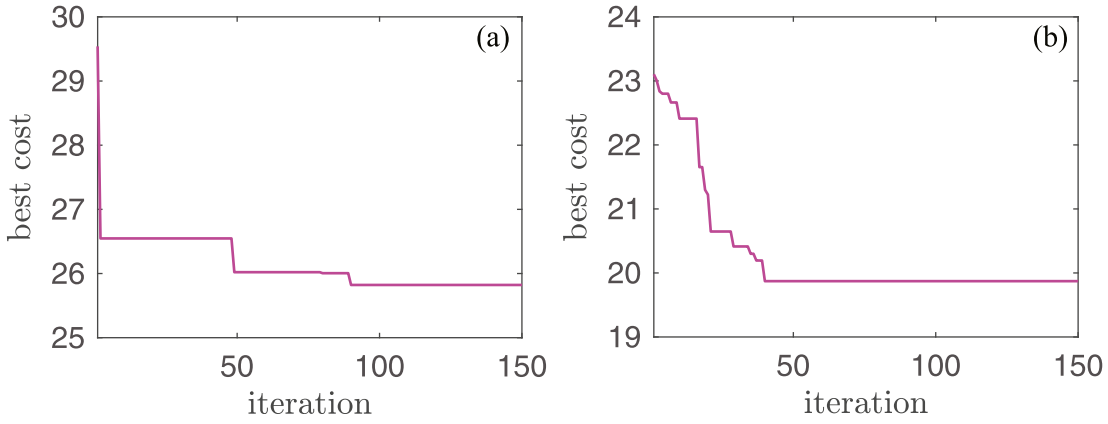

Fig. 5. The best costs vs. the iterations: (a) zone 2, and (b) zone 4.

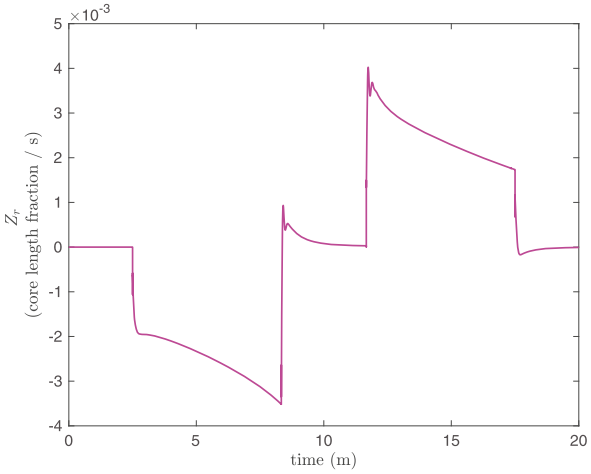

Fig. 6. Control rod speed (control signal).

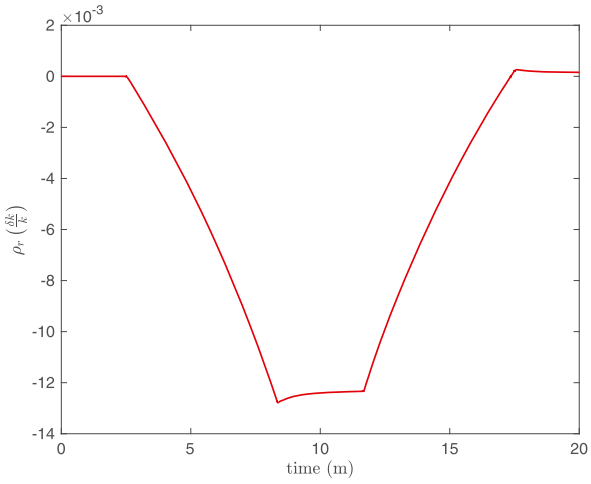

Fig. 7. Control rod reactivity.

4. Conclusion

A novel meta-heuristic algorithm called HGSO has been used to tune PID gains for a load-following operation of an NPP. This optimization algorithm is inspired by Henry's law. Meta-heuristic algorithms are not required experimental data, analytical calculations, or linearization methods, unlike other theoretical or experimental methods. In this optimization algorithm, the ITSE performance index was used as the objective (cost) function, which was constrained by a stability condition based on a Lyapunov synthesis. The simulation results revealed that HGSO has achieved significant superiority against an empirically tuned PID, without any computational cost. This method demonstrates good accuracy compared to a GA-tuned PID controller.

Declaration of competing interest

The authors declare that they have no known competing financial interests or personal relationships that could have appeared to influence the work reported in this paper.

References

[1] F.A. Hashim, E.H. Houssein, M.S. Mabrouk, W. Al-Atabany, S. Mirjalili, Henry gas solubility optimization: a novel physics-based algorithm, Future Generat. Comput. Syst. 101 (2019) 646–667.
[2] F.A. Hashim, E.H. Houssein, K. Hussain, M.S. Mabrouk, W. Al-Atabany, A modified Henry gas solubility optimization for solving motif discovery problem, Neural Comput. Appl. 32 (2020) 10759–10771.
[3] N. Neggaz, E.H. Houssein, K. Hussain, An efficient henry gas solubility optimization for feature selection, Expert Syst. Appl. 152 (2020) 113364.
[4] B.S. Yıldız, A.R. Yıldız, N. Pholdee, S. Bureerat, S.M. Sait, V. Patel, The Henry gas solubility optimization algorithm for optimum structural design of automobile brake components, Mater. Test. 62 (2020) 261–264.
[5] S. Ekinci, B. Hekimoğlu, D. Izci, Opposition based Henry gas solubility optimization as a novel algorithm for PID control of DC motor, Eng. Sci. Technol. an Int. J. 24 (2021) 331–342.
[6] S. Ekinci, D. Izci, B. Hekimoğlu, Henry gas solubility optimization algorithm based FOPID controller design for automatic voltage regulator, in: 2020 Int. Conf. Electr. Commun. Comput. Eng., 2020, pp. 1–6.
[7] S. Ekinci, D. İzci, B. Hekimoğlu, Implementing the Henry Gas Solubility Optimization Algorithm for Optimal Power System Stabilizer Design, 2021.
[8] D. İzci, S. Ekinci, Comparative performance analysis of slime mould algorithm for efficient design of proportional–integral–derivative controller, Electrica 21 (2021) 151–159.
[9] D. Izci, S. Ekinci, A. Demirören, J. Hedley, HHO algorithm based PID controller design for aircraft pitch angle control system, in: 2020 Int. Congr. Human-Computer Interact. Optim. Robot. Appl, IEEE, 2020, pp. 1–6.
[10] S. Ekinci, B. Hekimoğlu, Improved kidney-inspired algorithm approach for tuning of PID controller in AVR system, IEEE Access 7 (2019) 39935–39947.
[11] S.M.H. Mousakazemi, N. Ayoobian, G.R. Ansarifar, Control of the pressurized water nuclear reactors power using optimized proportional–integral–derivative controller with particle swarm optimization algorithm, Nucl. Eng. Technol. 50 (2018) 877–885.
[12] S.M.H. Mousakazemi, N. Ayoobian, G.R. Ansarifar, Control of the reactor core power in PWR using optimized PID controller with the real-coded GA, Ann. Nucl. Energy 118 (2018) 107–121.
[13] G. Kirui, J. Wang, Design of a fuzzy FOPID controller for power level control of a pressurized water reactor, ACM Int. Conf. Proc. Ser. 144 (2020) 549–553.
[14] M. Elsisi, H. Abdelfattah, New design of variable structure control based on

lightning search algorithm for nuclear reactor power system considering load-following operation, Nucl. Eng. Technol. 52 (2020) 544–551.
[15] B. Puchalski, T.A. Rutkowski, K. Duzinkiewicz, Fuzzy multi-regional fractional PID controller for pressurized water nuclear reactor, ISA Trans. 103 (2020) 86–102.
[16] A.A. de M. Meneses, L.M. Araujo, F.N. Nast, P.V. da Silva, R. Schirru, Application of metaheuristics to Loading Pattern Optimization problems based on the IAEA-3D and BIBLIS-2D data, Ann. Nucl. Energy 111 (2018) 329–339.
[17] J.J. Ortiz-Servin, D.A. Pelta, J.M. Cadenas, A. Castillo, J.L. Montes-Tadeo, Methodology for integrated fuel lattice and fuel load optimization using population-based metaheuristics and decision trees, Prog. Nucl. Energy 104 (2018) 264–270.
[18] P.A. Wrigley, P. Wood, P. Stewart, R. Hall, D. Robertson, Module layout optimization using a genetic algorithm in light water modular nuclear reactor power plants, Nucl. Eng. Des. 341 (2019) 100–111.
[19] D.W. Lim, C.W. Lee, J.Y. Lim, D. Hartanto, On the particle swarm optimization of cask shielding design for a prototype sodium-cooled fast reactor, Nucl. Eng. Technol. 51 (2019) 284–292.
[20] N. Zare, G. Jahanfarnia, A. Khorshidi, J. Soltani, Robustness of optimized FPID controller against uncertainty and disturbance by fractional nonlinear model for research nuclear reactor, Nucl. Eng. Technol. 52 (2020) 2017–2024.
[21] G. Wang, J. Wu, B. Zeng, Z. Xu, X. Ma, A nonlinear adaptive sliding mode control strategy for modular high-temperature gas-cooled reactors, Prog. Nucl. Energy 113 (2019) 53–61.
[22] N. Kastin, E. Meron, A. Kolin, S. Kinast, Nonlinear stability and limit cycles in xenon-induced reactor oscillations, Prog. Nucl. Energy 116 (2019) 168–179.
[23] D.L. Hetrick, Dynamics of Nuclear Reactors, American Nuclear Society, 1993.
[24] G.R. Ansarifar, M. Rafiei, Higher order sliding mode controller design for a research nuclear reactor considering the effect of xenon concentration during load following operation, Ann. Nucl. Energy 75 (2015) 728–735.
[25] R.A. Krohling, J.P. Rey, R.A. Krohling, J.P. Rey, Design of optimal disturbance rejection PID controllers using genetic algorithms, IEEE Trans. Evol. Comput. 5 (2001) 78–82.
[26] H.E.A. Ibrahim, F.N. Hassan, A.O. Shomer, Optimal PID control of a brushless DC motor using PSO and BF techniques, Ain Shams Eng. J. 5 (2014) 391–398.
[27] A. Dabiri, B.P. Moghaddam, J.A.T. Machado, Optimal variable-order fractional PID controllers for dynamical systems, J. Comput. Appl. Math. 339 (2018) 40–48.
[28] K. Zare, M.T. Hagh, J. Morsali, Effective oscillation damping of an interconnected multi-source power system with automatic generation control and TCSC, Int. J. Electr. Power Energy Syst. 65 (2015) 220–230.
[29] H. Gozde, M.C. Taplamacioglu, Automatic generation control application with craziness based particle swarm optimization in a thermal power system, Int. J. Electr. Power Energy Syst. 33 (2011) 8–16.
[30] K. Naidu, H. Mokhlis, A.H.A. Bakar, V. Terzija, H.A. Illias, Application of firefly algorithm with online wavelet filter in automatic generation control of an interconnected reheat thermal power system, Int. J. Electr. Power Energy Syst. 63 (2014) 401–413.
[31] K.J. Astrom, T. HÄgglund, Advanced PID Control, ISA-The Instrumentation, Systems and Automation Society, 2006.